Flow Science Report 04-14

FLOW-3D Core Gas Model: Binder Gas Generation and Transport in Sand Cores and Molds

A. J. Starobin and C. W. Hirt
Flow Science, Inc.
October 2009

Revised by: Liping Xue
Flow Science, Inc.
August 2014

Overview

The making of resin-bonded sand castings has made great strides in quality over its long history. Even so, there remain some process-related defects that are not fully understood and can cause quality issues. For instance, chemical binders in the sand can produce gas when heated by the molten metal and if not vented adequately, the gas may flow into the metal resulting in a gas porosity defect. This is most likely with cores that form thin interior features of castings that heat up quickly and have long venting paths. The core gas model in ***FLOW-3D***[1] is designed to predict the possibility of such gas defects and is intended to help design core venting that would evacuate safely all the binder product gas from the cores.

Two major types of binders are used in core making practice: resin-based organic binders and inorganic binders such as sodium silicate [1]. The organic binders are either thermosetting, or cured at room temperature with an aid of a catalyst. These are favored in many applications due to their complete degradation even at aluminum casting temperatures and for the ease of subsequent sand shake out. The core gas model is developed with these binders in mind, but can be extended to inorganic binders if appropriate data on their decomposition is available.

The Core Gas Model

The major factors contributing to core gas pressure are described by Campbell [2]. The hot product gas forms over a range of temperatures between 500 and 700 K for resin-based binders. The gas then flows toward the vents through porous sand with an associated pressure loss. The sand porosity can be as high as 40% [1]. Venting either occurs naturally at the back of the mold, or is introduced by drilling through the mold halves to the core print locations.

---

[1] ***FLOW-3D*** is a registered trademark in the USA and other countries.

The microscopic velocity of the core gas, $\vec{u}_{cg}$, is governed by the equation for flow in porous media:

$$\vec{u}_{cg} = -\frac{K}{\mu}\nabla p_{cg} \ , \qquad (1)$$

where K is the intrinsic sand permeability found to be approximately 10^{-10} m^2 in room temperature air flow experiments [3,10], μ is core gas viscosity and p_{cg} is the core gas pressure. The specific form of the drag coefficient, which is inversely proportional to permeability, is the same as in the ***FLOW-3D*** Reynolds-dependent drag model. The inertial term is found to be relatively small and is not included in Eq. (1). Furthermore, the possible compositional and temperature dependence of the gas viscosity is not accounted for.

The density of the core gas is governed by the mass transport equation:

$$\frac{\partial \rho_{cg}}{\partial t} + \nabla \cdot (\rho_{cg}\vec{u}_{cg}) = -\frac{d\rho_b}{dt}, \qquad (2)$$

where ρ_{cg} is the microscopic (mass per unit open volume) core gas density and ρ_b is the macroscopic (mass per unit bulk core volume) core binder density. The core gas is compressible. For example, even in the absence of gas sources there can be a thermal expansion and flow of the initial air in the core as the core heats up. Furthermore, while the pressures in the cores are expected to be above the ambient pressure and are effectively limited by the surrounding metal pressure, the temperature variations from the core surface to the vents can be as large as a factor of two suggesting a significant contraction of the core gas during flow.

The density transport equation, Eq. (2), must be numerically solved with an implicit coupling to the velocity equation to insure computational stability at reasonable time-step sizes. This is achieved by using a variant of the Implicit Continuous-fluid Eulerian (ICE) method [7].

The core gas density is further constrained by the ideal gas law which describes well the binder product gas, especially at high temperatures:

$$p_{\mathrm{cg}} = \mathrm{R}_{\mathrm{cg}}\rho_{\mathrm{cg}}T, \qquad (3)$$

The gas constant R_{cg} is estimated from calibration experiments, while the temperature of the gas is assumed to be equal to the local core temperature. This is a good approximation because of the high heat content of the solid core material compared to that of the gas and, additionally, due to the high surface area per unit bulk volume which is of the order of $10^4 m^{-1}$ [3] in core sands.

The conversion of the solid binder to gas is described by an Arrhenius relationship in accord with a number of previous thermal decomposition studies on polymers [4,5,12]:

$$\frac{d\rho_b}{dt} = -(\rho_b - \rho_{\text{res}})C_b\, e^{-\frac{E_b}{RT}}, \qquad (4)$$

where ρ_b is the solid binder density, ρ_{res} is the solid binder residue density, C_b is an empirical reaction rate constant, E_b is a component binding energy, R is the universal gas constant and T is the core temperature. The work in [5] is particularly useful for this approximation since the two reaction constants were determined for the pyrolysis of polyurethane resins at different heating rates. The two constants are 134 *kJ/mol* and $4.25\ 10^{10} s^{-1}$ and the reaction order is close to one hence the simple form of Eq. (4). The highest heating rate probed in this pyrolysis study was only 0.3 *deg/sec*, while at the core surface in iron immersions the heating rate can be as high as 80 *deg/sec*. However, at this point this is the best data available and it was used for the simulations described below.

Using the exponential Arrhenius rate for binder decomposition can introduce some undesirable computational effects. For example, for the decomposition law given by Eq. (4) with the listed reaction constants, most of the binder loss happens between 645 and 700 *K*. Given the steep temperature gradient of about 10^5 *K/m* at the core surface adjacent to liquid iron, even at mesh resolutions as fine as 2 *mm* the change in temperature between a surface cell and its neighbor in the core interior is larger than the decomposition zone width. Thus, at this mesh resolution, the source may exhibit an unphysical oscillatory behavior associated with the discrete size of the computational elements. To alleviate this problem, a simple subdivision scheme is used in each computational cell. The sub-cells store the solid binder density, while the sub-cell temperature is obtained through a linear interpolation from the temperature in the coarser main grid.

Two additional simplifying assumptions are made in the core gas model. First, no gas is allowed to condense within the core. For most practical cases, condensation, if it occurs, is not likely to significantly affect the gas pressure at early stages of the process when it is the principal source for gas-related casting defects. Second, the possible endo- or exo-thermic effects of the pyrolytic binder decomposition are also ignored.

When the core gas model is used concurrently with a mold filling simulation, gas flow in the cores may become sufficiently fast to limit the computational time-step size by the Courant stability condition for the explicit advection approximation to a value smaller than what is needed for the metal flow, resulting in longer calculation times. A sub-time-stepping scheme has been incorporated into the core gas model to remove this limitation.

This is possible because the core gas model is coupled to metal flow only through the boundary conditions at the core surface (see the Core Boundary Conditions section). If the time-step size stability limit for the core gas model becomes smaller than that for the filling simulation, then the time-step size for the core gas computations is further reduced to a value that is an integer fraction of the global time step. The gas flow equations are then integrated over that number of steps to bring the solution forward to the end of the current global time step. The core gas computations are usually much faster compared to those for the filling because the gas dynamics is simpler and the core gas region occupies only a portion of the full simulation domain.

Since the core gas solution is only solved over the core, in the model implementation, a core-gas solution sub-domain is introduced, which only includes the core gas cells and needed boundary cells. The result is a much more compact and efficient representation of the solution in memory, shorter simulation times, and smaller `flsgrf` output files. Special data writing and retrieving algorithms are also introduced for core gas quantities, such that for restart simulation, even with different mesh and number of core gas sub-cells, the solution can be correctly retrieved from the restart source file. Finally, the core gas solver has been SMP parallelized.

Core Boundary Conditions

At the outer boundaries of the core material there may be a flow of gas either in or out of the core. If there is no metal at the core surface the gas is free to pass in either direction, and the surface pressure is equal to the ambient pressure in the mold. When there is metal at the core surface the following simplified mechanical pressure balance is used:

$$p_{cg} \leq p_m, \qquad (5)$$

in other words, gas is allowed to escape (blow) into the metal when the gas pressure, p_{cg}, exceeds the metal pressure outside, p_m, but metal cannot penetrate the core.

Equation (5) ignores a possible contribution of metal surface tension and any pressure loss associated with the penetration of oxide/solid skin at the core-metal interface. However, in this form the model gives the worst case scenario for the amount of gas blow into the metal. If the solid fraction in the metal at the surface is above a small cutoff it was assumed that a solid skin has formed at the core surface and no binder gas can escape at that location, i.e., the core is sealed at this location.

Another boundary condition is applied at print surfaces, that is, where a core surface is in contact with another solid part of the mold. In the actual castings the gas does not normally escape unless channels are cut into the mold to allow for venting. The core gas model has an option for allowing venting at print surfaces. If this option is activated, the print pressure is set to the initial ambient pressure in the mold.

Calibration Experiments and Simulations

The experimental techniques that quantify the amount of binder gas can be broadly classified as displacement [8,9] or as pressure-based methods [10]. In the former, the collected gas displaces oil in a tank with the back of the tank vented to the ambient pressure. In the latter, the gas is collected in a fixed volume apparatus and the gas pressure is measured. In both cases the collection lines are kept at an elevated temperature to prevent condensation of the volatile components which contribute to core pressure. In both cases the standard volumetric rate of the product gas is reported over time.

Data obtained by the pressure-based method was used to calibrate the present model. In this test we assume that the binder converts completely into gas. The gas is thought to be ideal and of fixed composition with the gas constant, R_{cg}. The gas constant is deduced from the total collected standard volume,V_{std}, the gas pressure and temperature, p_{std} and T_{std}, and the initial mass of the binder, m_b:

$$R_{cg} = \frac{p_{std}}{T_{std}} \frac{V_{std}}{m_b}, \tag{6}$$

The apparatus schematic is shown in Fig. 1 on the left. The holder and the core are immersed into a crucible with iron at 1700 *K* over a time of approximately 4 seconds. The core is then held submerged until no more gas is collected in the apparatus and the gas pressure in the collection chamber is no longer changing. The full binder pyrolysis time is approximately 110 *sec* and about 840 *cc* of standard volume gas is collected. The peak in gas volume evolution is recorded at approximately 3 seconds and is 44 *cc/sec*.

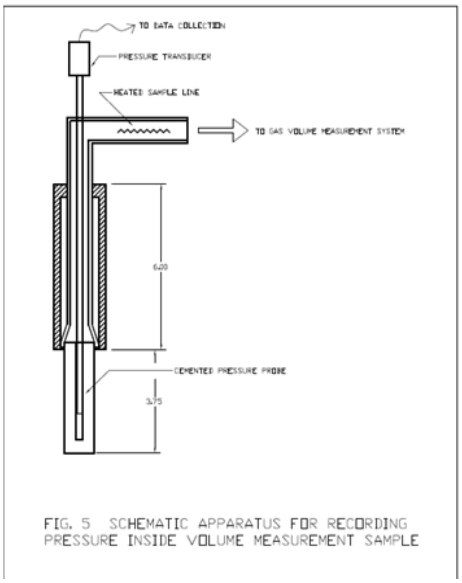

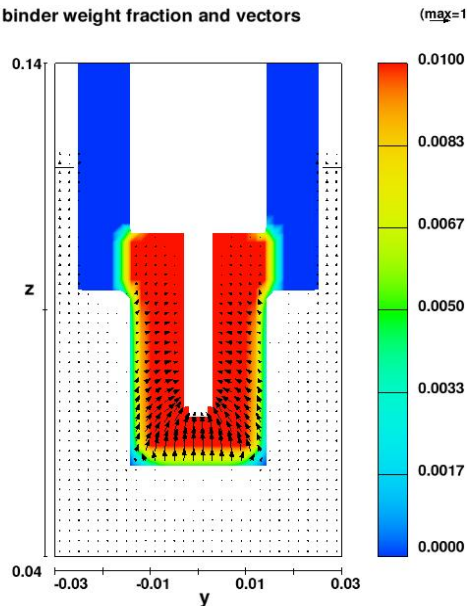

Figure 1. Left Panel: the schematic of the gas collection apparatus of Alchemcast [10]. The holder and the calibration core 51 *mm* long and 28.6 *mm* in diameter are immersed into the crucible with molten metal, and the binder gas is collected at the top through a line kept at 366.5 *K*, where the gas pressure is monitored. Right Panel: simulated calibration experiment with a 4 *sec* immersion time. At the end of immersion the binder has pyrolysed primarily at the core surface.

This data is sufficient to calculate the gas constant using Eq. (6). It is approximately 494 *J/mol/K* for the product gas resulting from PUCB pyrolysis. The remaining data required

for the calibration simulation was measured at Alchemcast [10] and is summarized in Table 1. The resulting simulated volumetric rate and integrated volume curve are plotted together with the measured quantities in Fig. 2. Overall, the agreement is good, with the peak time captured accurately and the peak rate somewhat underestimated. There is some evidence [1,6] that composition of collected gas varies from light to heavy during the casting process, the inclusion of which may further improve the agreement between data and simulation. However, variable gas composition is beyond the scope of the current model. The shape of the pyrolysis zone near the peak time is shown in Fig. 1 on the right, and it is evident that the core surface binder is primarily responsible for the outgassing peak.

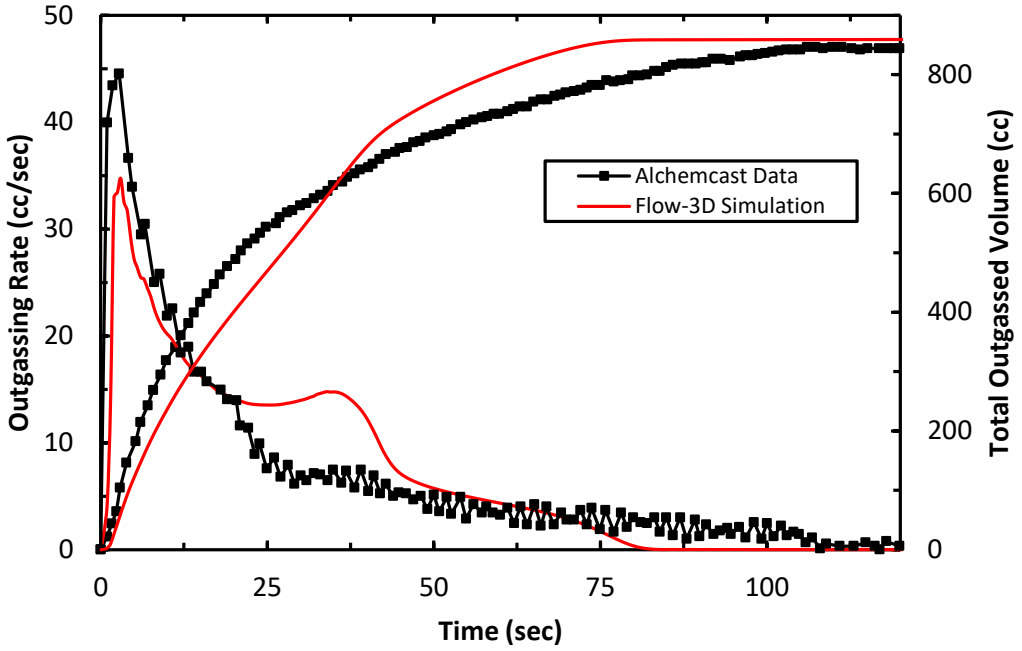

Figure 2. Calibration data (black lines with symbols) for the core sample shown in Fig. 1 immersed in Iron (1700 *K*) and results from the ***FLOW-3D*** core gas model (smooth, red lines). The model captures well the peak time and rate of gas generation, and tracks well the shape of the outgassing curve.

Table 1. Suggested Properties for Resin-Bonded Cores

Core Porosity	0.39
Core Permeability (m^2)	2.4154e-11
Core Density (kg/m^3)	1470
Binding Energy (*J/mol*)	134e3
Decomposition Rate (1/*sec*)	4.25e10
Binder Gas Constant (*J/kg/K*)	494
Core Gas Viscosity (*Pa sec*)	1.7e-5

The calibration simulation was performed on a 1 *mm* mesh. Since the pyrolysis zone width is much thinner (about 0.25 *mm* in PUCB in iron immersions) the sub-scaling dimension for the binder variable is chosen to be 4 in each coordinate direction. The effect of the sub-scaling dimension on the accuracy of the computation is explored in Fig. 3.

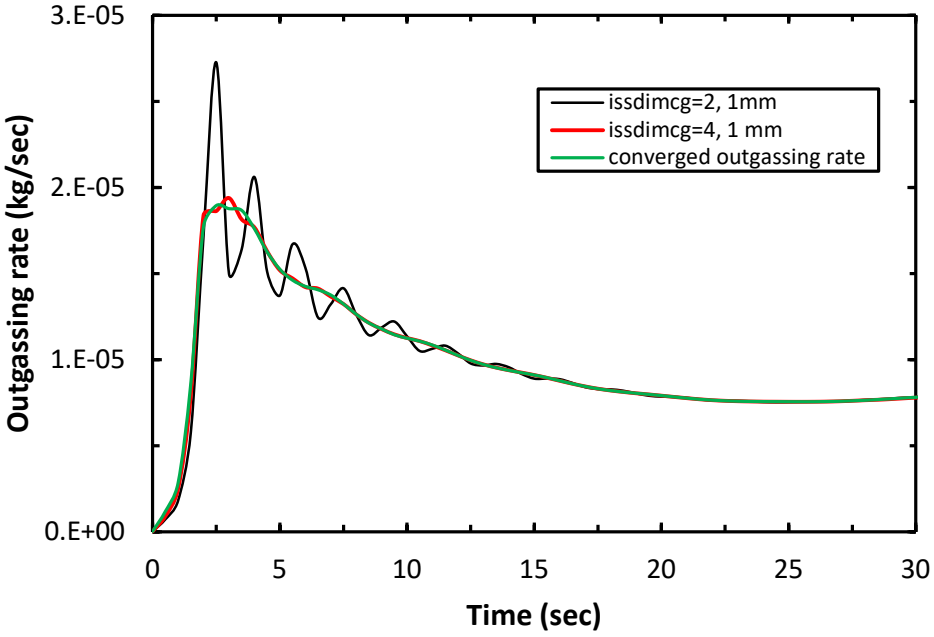

Figure 3. The sub-scale dimension of the binder fraction field affects the accuracy of the computed outgassing rates and gas pressures. Shown are the converged outgassing history (smooth green line), outgassing history with the sub-scale dimension of 4 and at mesh resolution of 1 *mm* (thick red line) and, finally, the outgassing history with a sub-scale dimension of 2 at mesh resolution of 1 *mm* (thin black line). Best accuracy is obtained when the sub-scale resolution is near the width of the pyrolysis zone estimated in iron castings to be ~ 0.25 *mm.*

A Sample Industrial Use of the Model

To further demonstrate the utility of the core gas model we show some results for an iron casting with two internal sand cores. The parameters used for the simulation are the same as in the previous section. The two internal cores contain 3 wt % of shell-resin. The full casting also includes a two-piece shell mold, however, only the internal cores in their correct relative orientation were simulated.

The simulation domain is bottom-filled at a rate corresponding to the fill time of the actual casting, which is 1.5 *sec*, using a time-dependent pressure boundary condition at the inlet. At the end of filling, the slope of the inlet pressure ramp increases, reaching the pressure head in the sprue. The actual sprue (not included in the model) is 230 *mm* tall. In the model, the inlet pressure at the end of filling corresponds to the sprue height of 150

mm. This is done to reduce the metal pressure at the end of filling and allow some gas to escape from the core into the metal for a demonstration purpose. The inlet boundary pressure history is plotted in Fig. 4.

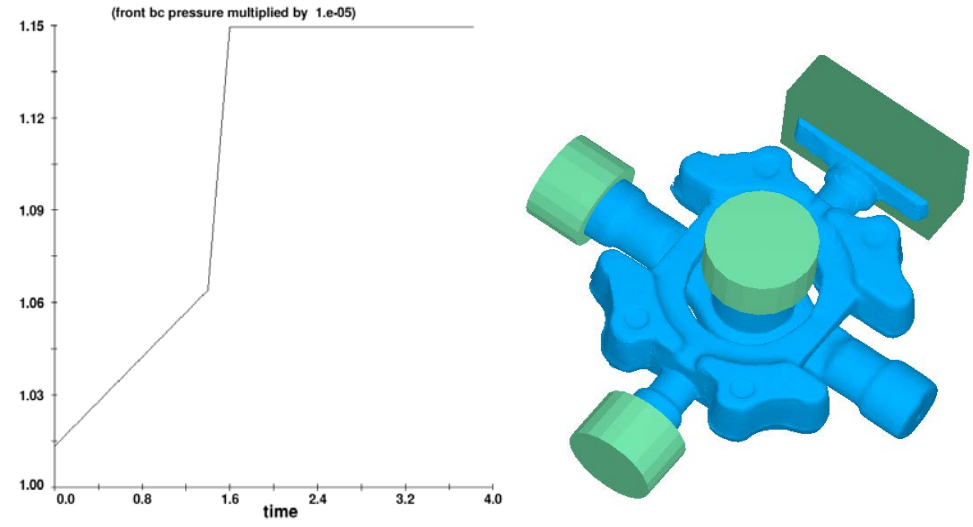

Figure 4. Left Panel: inlet pressure history for the metal at the bottom of the simulation domain. Domain height is ~ 90 *mm*. Right Panel: the geometry of the two internal cores. The ring, or "saddle" core, in the horizontal plane is proximate, but does not touch the vertical T-core. The green pads indicate the locations of vented prints into the shell mold. The right side of the horizontal bar on the T-core is printed, but the print has no explicit venting. Also, there is an additional center drill vent from the top print of the T-core that reaches roughly to the center of that core.

The core geometry and vented print locations are also shown in Fig. 4. An additional center drill vented into the T-core is not visible. In this venting configuration the findings are summarized in Fig. 5, where the core gas pressure (left) and surface gas mass flux (right) are shown at 5 *sec* from the start of the filling. It is clear that the T-core is adequately vented and the center drill vent is essential for evacuating the gas from the T-core. The saddle core on the other hand is not vented sufficiently and continues to blow gas into the metal at its top surface 3.5 seconds after the end of fill. The peak pressure in the saddle core, ~ 10 *kPa* above the ambient, is twice that of the gas in the T-core and is essentially equal to the hydrostatic metal pressure around it. An additional 50 *mm* in sprue height would suppress gas blow after the end of filling, but the saddle core will continue to blow significant amount of gas during the fill.

Summary

A model for the binder gas generation and transport in sand cores and molds based on first principles has been added to ***FLOW-3D***. The model was implemented numerically in an efficient fashion, allowing engineers to use it in combination with other models in ***FLOW-3D***, such as metal flow and solidification. The core gas model give engineers the

means to validate casting designs with respect to the possibility of gas blow into the metal. Different venting and filling scenarios can be evaluated.

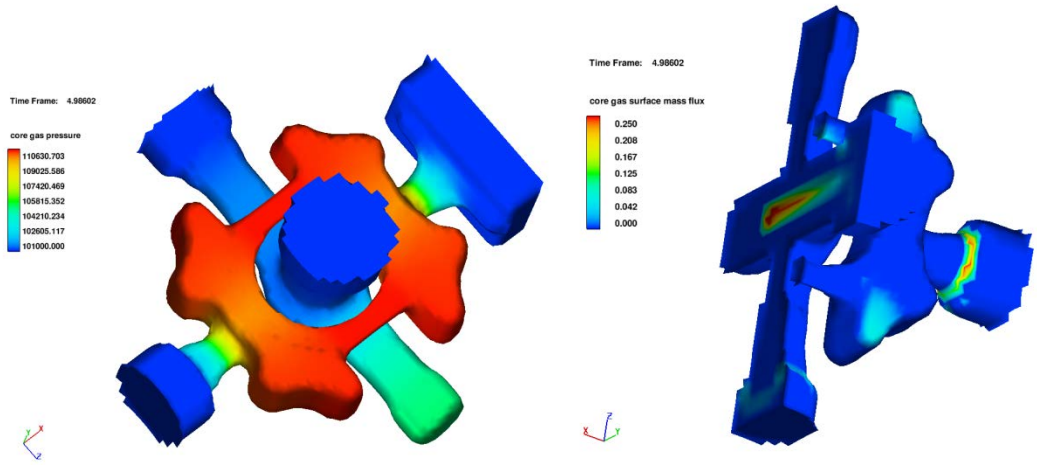

Figure 5. Contour plots of gas pressure (left) and gas surface mass flux (right) to metal at 5 *sec*. In order to clearly show the binder gas venting by the center vertical drill, for the gas surface mass flux contour, the T-core is shown cut through the middle. The filling time is 1.5 *sec*. The gas pressure in the saddle core is roughly double what it is in the T-core. The vertical drill in the T-core along with one T-core print is very effective in venting all the T-core binder gas. The saddle core remains inadequately vented in this design.

Acknowledgments

The development effort has greatly benefited from experimental input from Dr. Charles Bates and David Burch of Alchemcast LLC and Dr. David Goettsch of General Motors. Additional thanks are to Harry Littleton, Amanda Hayes of Alchemcast LLC and Libby Rider of Graham-White Manufacturing Co. A portion of this technical note was published in [13] where other industrial validations can be found.

References

1. WD Scott, Hanjun Li, John Griffin, and Charles Bates, “Production and Inspection of Quality Aluminum Castings,” in Handbook of Metallurgical Process Design, edited by G. Totten, 2004

2. J. Campbell, *Castings* (Butterworth-Heinemann, 2000), 105-109

3. Donald A. Nield and Adrian Bejan, *Convection in Porous Media* (Springer, 2006), 5, 39-40

4. Kalayan Annamalai and Ishwar K. Puri, *Combustion Science and Engineering* (CRC Press, 2007), 390-391

5. R. Font et. al., "Pyrolysis study of polyurethane," *Journal of Analytical and Applied Pyrolysis*, 58-59, (2001), 63-77

6. W.D. Scott and C.E. Bates, "Decomposition of resin binders and the relationship between gases formed and the casting surface quality," *AFS Transactions*, 1980

7. Harlow, F.H. and Amsden, A.A., "A Numerical Fluid Dynamics Calculation Method for All Flow Speeds," *J. Comput. Phys*. **8**, 197 (1971)

8. J. Orlenius, U. Gotthardsson and A. Dioszegi, *ibid* "Mould and Core Gas Evolution in Grey Iron Castings," *International Journal of Cast Metals Research*, 2008, in press

9. L. Winardi, R.D. Griffin, H.E. Littleton, J.A. Griffin, "Variables Affecting Gas Evolution Rates and Volumes from Cores in Contact with Molten Metal," *AFS Transactions* **116**, 505-521, 2007

10. AlchemCast LLC, Pelham, Alabama, USA, www.alchemcast.com

11. ***FLOW-3D***® *Theory Manual*, (Flow Science Inc., Santa Fe, New Mexico, USA, www.flow3d.com , 2009).

12. Lengelle, G., "Thermal Degradation Kinetics and Surface Pyrolysis of Vinyl Polymers," AIAA J., 8(11), 1989-1196, 1970

13. Andrei Starobin, C.W. Hirt, D. Goettsch, "A Model for Binder Gas Generation and Transport in Sand Cores and Molds," http://www.flow3d.com/pdfs/tp/cast_tp/FloSci-Bib19-09.pdf, Modeling of Casting, Welding, and Solidification Processes XII, TMS (The Minerals, Metals & Minerals Society), June 2009